

# Mutations Affecting the SAND Domain of DEAF1 Cause Intellectual Disability with Severe Speech Impairment and Behavioral Problems

Anneke T. Vulto-van Silfhout,<sup>1,14</sup> Shivakumar Rajamanickam,<sup>2,14</sup> Philip J. Jensik,<sup>2,14</sup> Sarah Vergult,<sup>3</sup> Nina de Rocker,<sup>3</sup> Kathryn J. Newhall,<sup>4</sup> Ramya Raghavan,<sup>2</sup> Sara N. Reardon,<sup>2</sup> Kelsey Jarrett,<sup>2</sup> Tara McIntyre,<sup>2</sup> Joseph Bulinski,<sup>2</sup> Stacy L. Ownby,<sup>2</sup> Jodi I. Huggenvik,<sup>2</sup> G. Stanley McKnight,<sup>4</sup> Gregory M. Rose,<sup>2,5</sup> Xiang Cai,<sup>2</sup> Andy Willaert,<sup>3</sup> Christiane Zweier,<sup>6</sup> Sabine Endeke,<sup>6</sup> Joep de Lig,<sup>1</sup> Bregje W.M. van Bon,<sup>1</sup> Dorien Lugtenberg,<sup>1</sup> Petra F. de Vries,<sup>1</sup> Joris A. Veltman,<sup>1</sup> Hans van Bokhoven,<sup>1,7</sup> Han G. Brunner,<sup>1</sup> Anita Rauch,<sup>8,9,10</sup> Arjan P.M. de Brouwer,<sup>1,7</sup> Gemma L. Carvill,<sup>11</sup> Alexander Hoischen,<sup>1</sup> Heather C. Mefford,<sup>11</sup> Evan E. Eichler,<sup>12,13</sup> Lisenka E.L.M. Vissers,<sup>1</sup> Björn Menten,<sup>3</sup> Michael W. Collard,<sup>2,15</sup> and Bert B.A. de Vries<sup>1,15,\*</sup>

Recently, we identified in two individuals with intellectual disability (ID) different de novo mutations in *DEAF1*, which encodes a transcription factor with an important role in embryonic development. To ascertain whether these mutations in *DEAF1* are causative for the ID phenotype, we performed targeted resequencing of *DEAF1* in an additional cohort of over 2,300 individuals with unexplained ID and identified two additional individuals with de novo mutations in this gene. All four individuals had severe ID with severely affected speech development, and three showed severe behavioral problems. *DEAF1* is highly expressed in the CNS, especially during early embryonic development. All four mutations were missense mutations affecting the SAND domain of DEAF1. Altered DEAF1 harboring any of the four amino acid changes showed impaired transcriptional regulation of the *DEAF1* promoter. Moreover, behavioral studies in mice with a conditional knockout of *Deaf1* in the brain showed memory deficits and increased anxiety-like behavior. Our results demonstrate that mutations in *DEAF1* cause ID and behavioral problems, most likely as a result of impaired transcriptional regulation by DEAF1.

## Introduction

Intellectual disability (ID) is a highly heterogeneous disorder that is frequently caused by de novo gene mutations.<sup>1–4</sup> Hence, exome sequencing of the individuals involved and their parents (trio approach) is an effective way of identifying the underlying cause. Recently, we and others showed that in 16%–31% of individuals with ID, mutations in genes associated with ID could be identified via trio-based exome sequencing.<sup>1,2,4,5</sup> In an additional ~20% of these individuals, a de novo mutation was identified in a candidate gene that was not previously associated with ID.<sup>1,2,4</sup> For these candidate genes associated with ID, it is often difficult to determine whether the de novo mutation is causative for the ID phenotype. To establish their role in an ID phenotype, it is essential to identify other individuals with both de novo mutations in the same gene and a similar phenotype and/or to perform functional assays to assess the effect of the amino acid change on the respective protein. For one of these

candidate genes, DEAF1 transcription factor (*DEAF1* [MIM 602635; RefSeq accession number NM\_021008.2]), de novo mutations were identified in two independent studies in two unrelated individuals with severe ID.<sup>2,4</sup>

*DEAF1* encodes deformed epidermal autoregulatory factor 1 homolog (DEAF1), a transcription factor that binds to TTCG motifs in DNA.<sup>6</sup> It is involved in the regulation of various genes,<sup>7</sup> including itself, as both a transcriptional activator<sup>8–10</sup> and a repressor.<sup>11,12</sup> DEAF1 comprises multiple structural domains: a SAND (Sp-100, AIRE, NucP41/75, and DEAF1) domain, which is essential for DNA binding (via its KDWK motif) and protein-protein interactions;<sup>11,13,14</sup> a MYND (myeloid translocation protein 8, Nery, and DEAF1) domain, which is a cysteine-rich module also involved in protein-protein interactions;<sup>15,16</sup> and a nuclear localization signal and a nuclear export signal important for nuclear localization of DEAF1.<sup>6</sup> A region within the nuclear export signal and another in the SAND domain also mediate DEAF1 multimerization, which is required for DNA binding.<sup>15,17</sup> Disruption of *Deaf1* in

<sup>1</sup>Department of Human Genetics, Radboud University Medical Center, 6500 HB Nijmegen, the Netherlands; <sup>2</sup>Department of Physiology and Center for Integrated Research in Cognitive & Neural Sciences, Southern Illinois University School of Medicine, Carbondale, IL 62901, USA; <sup>3</sup>Center for Medical Genetics, Ghent University, Ghent 9000, Belgium; <sup>4</sup>Department of Pharmacology, University of Washington, Seattle, WA 98195, USA; <sup>5</sup>Department of Anatomy, Southern Illinois University School of Medicine, Carbondale, IL 62901, USA; <sup>6</sup>Institute of Human Genetics, Friedrich-Alexander-Universität Erlangen-Nürnberg, 91054 Erlangen, Germany; <sup>7</sup>Department of Cognitive Neurosciences, Radboud University Medical Center, 6500 HB Nijmegen, the Netherlands; <sup>8</sup>Institute of Medical Genetics, University of Zurich, 8603 Schwerzenbach-Zurich, Switzerland; <sup>9</sup>Neuroscience Center Zurich, University of Zurich, 8603 Schwerzenbach-Zurich, Switzerland; <sup>10</sup>Zurich Center of Integrative Human Physiology, University of Zurich, 8603 Schwerzenbach-Zurich, Switzerland; <sup>11</sup>Division of Genetic Medicine, Department of Pediatrics, University of Washington, Seattle, WA 98195, USA; <sup>12</sup>Department of Genome Sciences, University of Washington School of Medicine, Seattle, WA 98195, USA; <sup>13</sup>Howard Hughes Medical Institute, Seattle, WA 98195, USA

<sup>14</sup>These authors contributed equally to this work

<sup>15</sup>These authors contributed equally to this work

\*Correspondence: [bert.devries@radboudumc.nl](mailto:bert.devries@radboudumc.nl)

<http://dx.doi.org/10.1016/j.ajhg.2014.03.013>. ©2014 by The American Society of Human Genetics. All rights reserved.

animal models produces neural-tube defects in mice<sup>18</sup> and early embryonic arrest in *Drosophila*.<sup>19</sup> In humans, *DEAF1* has previously been associated with major depression and suicide,<sup>20–22</sup> autoimmune disorders,<sup>7</sup> and cancer.<sup>8,23</sup>

Here, we aimed to determine whether de novo mutations affecting the SAND domain of *DEAF1* could be the underlying cause of ID in humans by (1) identifying and deeply phenotyping multiple individuals with de novo mutations in *DEAF1*, (2) assessing the effect of the human amino acid substitutions on *DEAF1* function, and (3) studying the phenotypic effect of the disruption of *Deaf1* in a mouse model. The results show that mutations affecting the SAND domain of the transcription factor *DEAF1* might lead to ID with severely affected expressive speech and behavioral abnormalities.

## Subjects and Methods

### Identification of Individuals with *DEAF1* Mutations

Targeted resequencing of the coding sequence of *DEAF1* was performed in two cohorts of individuals with unexplained ID. The first cohort of 765 individuals was resequenced after targeted array-based enrichment as described before,<sup>1</sup> whereas the second cohort of 1,561 individuals was assayed with molecular inversion probes (MIPs) as described previously.<sup>24</sup> Both of these cohorts were selected from the in-house collection of the Department of Human Genetics of Radboud University Medical Center (Nijmegen) and consisted of over 5,000 samples from individuals with unexplained ID. Candidate mutations were tested by standard Sanger sequencing approaches on DNA extracted from peripheral blood. For assessing the de novo occurrence of confirmed mutations, DNA from the parents was tested. This study was approved by the institutional review board Commissie Mensgebonden Onderzoek Regio Arnhem-Nijmegen NL36191.091.11. Written informed consent was obtained from all individuals.

### Assessment of *DEAF1* Expression

*DEAF1* expression was assessed in different human fetal and adult tissues and in mouse brain by quantitative PCR (qPCR). In addition, the expression of the *DEAF1* orthologs *deaf1-a* (zgc:194895) and *deaf1-b* (zgc:171506) in zebrafish was assessed by in situ hybridization and qPCR at different time points.

### Assessment of Altered *DEAF1*

#### *Plasmids and Site-Directed Mutagenesis*

*DEAF1* mammalian expression plasmids in pcDNA3 and fused in-frame to a carboxy-terminal FLAG epitope tag were derived from the human *DEAF1* cDNA (GenBank accession number AF049459) and have been previously described.<sup>11,15</sup> Site-directed mutagenesis to introduce the p.Arg224Trp (c.670C>T), p.Ile228Ser (c.683T>G), p.Gln264Pro (c.791A>C), and p.Arg254Ser (c.762A>C) amino acid substitutions into the *DEAF1* expression plasmids were generated by PCR using primers containing the indicated human amino acid substitutions. Primers also contained specific *DEAF1* native restriction endonuclease sites to facilitate subcloning. Digested PCR fragments were used to replace the corresponding regions of wild-type (WT) *DEAF1*. The reporter plasmid pDEAF1pro-luciferase is similar to the previously described pNUDRproCAT6<sup>11</sup> and was

constructed by subcloning of the 1,150 bp region 5' to the ATG start codon of the human *DEAF1* promoter into the pGL3 basic firefly luciferase reporter plasmid (Promega). The mouse *Eif4g3* promoter region from –609 to +58 (relative to the transcription start site) was amplified from mouse genomic DNA by PCR (primers are in [Table S1](#), available online), and the product was subcloned into the *NheI* and *HindIII* sites of the pGL3 basic plasmid. All plasmid constructs were confirmed by DNA sequencing by a Beckman Coulter CEQ 8000 Genetic Analysis System.

#### *Transcription Assay*

Human embryonic kidney 293T (HEK293T) cells were plated in 24-well plates (90,000 cells per well) and transfected with 125 ng pcDNA3 (control) or *DEAF1* (expressing WT or altered *DEAF1*) expression plasmids, along with 375 ng pDEAF1pro-luciferase or pEif4g3pro-luciferase and 1.25 ng Rous sarcoma virus (RSV)-*Renilla* (for normalization), via the calcium phosphate technique. Media were replaced 18 hr later, and luciferase assays were performed 24 hr later with the Dual-Luciferase Reporter Assay System (Promega) according to the manufacturer's protocol.

#### *Purification of Recombinant FLAG-Tagged Proteins*

HEK293T cells were transfected with 10 µg of expression plasmids for WT or altered FLAG-tagged *DEAF1*. Cell lysates were prepared in lysis buffer P (150 mM NaCl, 50 mM Tris, pH 7.5, 1 mM EDTA, 1% Triton X-100, 1 mM DTT, 1 mM NaF, and Complete Protease Inhibitor Cocktail [Roche]) on ice, and cell debris were removed by centrifugation. Lysates were incubated with anti-FLAG beads overnight at 4°C. Proteins bound to the beads were washed four times with lysis buffer P and once with Tris-buffered saline (TBS: 50 mM Tris, pH 7.4, and 150 mM NaCl) before elution with 200 ng/ml FLAG in TBS for 30 min on ice and then the addition of glycerol to 50%. Protein concentrations were calculated by Coomassie blue staining and comparison to BSA standards after SDS-PAGE ([Figure S1](#)). Band intensities were quantified on a Li-Cor Odyssey CLx.

#### *GST Pull-downs to Examine *DEAF1* and *XRCC6* Interactions*

Glutathione S-transferase (GST) and GST-*XRCC6* fusion proteins were purified as previously described.<sup>14</sup> FLAG-tagged WT and altered *DEAF1* were purified from transfected HEK293T cells as previously described (see above and [Jensik et al.<sup>14</sup>](#)). Five hundred nanograms of GST or GST-*XRCC6* attached to glutathione beads was incubated with 100 ng of purified WT or altered FLAG-tagged *DEAF1* in interaction buffer (50 mM NaCl, 20 mM Tris, pH 7.9, 0.1% Nonidet P-40, 10% glycerol, 1 mM dithiothreitol, and 0.25% BSA) overnight at 4°C. Beads were then washed six times with interaction buffer, and proteins were eluted from beads with Laemmli sample buffer. Eluted samples and similar amounts of purified FLAG-tagged *DEAF1* used in the GST pull-down (inputs) were separated on SDS-PAGE gels and transferred to polyvinylidene fluoride membrane. Immunoblot analysis was then performed with an anti-*DEAF1* antibody.<sup>6</sup>

#### *Electrophoretic Mobility Shift Assays*

For electrophoretic mobility shift assays (EMSA), we used full-length recombinant *DEAF1* isolated from HEK293 cells ([Figure S1](#)) and two DNA ligands for *DEAF1*—the first consisted of two TTCC motifs spaced by 11 nucleotides and was based on a sequence found in the human *DEAF1* promoter,<sup>11,12</sup> and the second had two TTCC motifs spaced by 6 nucleotides. This latter sequence was a high-affinity ligand and was based on the preferred binding motif of *DEAF1* (data not shown). Fluorescently labeled double-stranded DNA (dsDNA) probes with 11 or 6 bp spacing of CG dinucleotides were generated by hybridization of oligonucleotides N52-69F and N52-69R or S6conF and S6conR, respectively

(Table S1). Oligonucleotides were labeled at their 5' ends with IRDye800 (N52-69) or IRDye700 (S6con) and purified by high-performance liquid chromatography (Integrated DNA Technologies). WT and altered FLAG-tagged DEAF1 from HEK293T cells (850 fmol) were incubated with 500 fmol of dsDNA probe and 1  $\mu$ g of poly(dA-dT) (nonspecific competitor) in a 20  $\mu$ l reaction containing 70 mM KCl, 35 mM Tris, pH 7.5, 0.7 mM DTT, 1 mM MnSO<sub>4</sub>, 2% (v/v) glycerol, and 100 U of lambda protein phosphatase (New England Biolabs) for 20 min at 25°C. Protein-DNA complexes were separated as previously described,<sup>11</sup> and band intensities were quantified on a Li-Cor Odyssey CLx.

#### Subcellular Localization

HEK293T cells on 35 mm dishes were cotransfected with 500 ng of expression plasmids for WT or altered FLAG-tagged DEAF1 and 500 ng pcDNA3 or hemagglutinin (HA)-tagged p.Lys304Thr DEAF1 expression plasmids via the calcium phosphate technique. Twenty-four hours later, cells were fixed in paraformaldehyde, permeabilized in methanol, and incubated with rabbit anti-HA (1:1,000 Santa Cruz) and mouse anti-FLAG (1:1,000 Sigma Aldrich) antibodies followed by Alexafluor-488-conjugated goat anti-rabbit IgG and Cy3-conjugated donkey anti-mouse IgG. Cells were visualized with an Olympus BW50 fluorescence microscope with a 60 $\times$  water objective.

### Generation of Mouse Knockout Models for *Deaf1*

Mice with a targeted disruption of exons 2–5 of *Deaf1*<sup>+/-</sup> (mice) were produced (Figure S3) and then backcrossed onto a C57BL/6 background for seven generations before F1 crosses were performed. In addition, a conditional knockout of *Deaf1* in mouse brain was produced with mice with loxP sites flanking exons 2–5 of *Deaf1* ("floxed," *Deaf1*<sup>+/-</sup> mice) (Figure S3). These were bred to congenic status onto a C57BL/6 background and were then bred to mice transgenic for nestin-cre (*Nes-cre*); these latter mice express Cre recombinase in neuronal and glial precursors by embryonic day 11.<sup>25</sup> Subsequent breeding produced mice with the genotype *Deaf1*<sup>fl/fl;Nes-cre</sup>, resulting in neuronal homozygous knockout (NKO) of *Deaf1* (these mice are hereafter referred to as NKO mice). Mice with a single conditional *Deaf1* allele and positive for *Nes-cre* have the genotype *Deaf1*<sup>+/-</sup>;Nes-cre. Mice with any combination of WT or floxed *Deaf1* alleles but lacking *Nes-cre* are referred to as control mice. Detailed protocols and supporting data for these procedures are provided in the Supplemental Data.

### Phenotyping of Mice with Conditional Targeting of *Deaf1*

Mice were tested for anxiety with the elevated plus maze (EPM) and the open-field test. The EPM tests for an animal's conflict between exploration and fear of open and/or elevated places. The EPM consists of two opposed closed arms (44  $\times$  6 cm) with raised walls (18 cm high) crossing with two open arms (44  $\times$  6 cm) without walls. A central platform (6  $\times$  6 cm) links the open and closed arms. The apparatus is elevated to a height of 55 cm from the floor. A mouse is placed in the central platform and allowed to explore the maze for 5 min, and movements are recorded with a digital camera and computer and analyzed with the ANY-maze software program (San Diego Instruments) for time spent and distance traveled. Open-field exploration also tests for unconditioned behavior and is designed to evaluate the total amount and rate of movement and the type of spontaneous activity and to provide a partially specific measure of anxiety-related behavior. The equipment consists of an open box (58  $\times$  58 cm), and the

animal is placed in the central arena, from which it is free to explore the box for 5 min. Mice prefer to stay near the walls of the box and avoid the center zone, which induces the conflict. Reduced time spent and distance traveled in the center zone is indicative of increased anxiety-like behavior in mice. Paths were recorded and analyzed with ANY-maze software.

The EPM and the open-field test were performed from 10 a.m. to 3 p.m. with constant illumination (50 lux). Between animals, testing surfaces were wiped with 70% ethanol followed by distilled water and then dried completely.

Learning and memory were tested with the Morris water maze and fear-conditioning tests. A white, circular tank 1 m in diameter and 30 cm deep was filled with 22°C–24°C water to a depth of 20 cm. Mice were tested in the water maze for 9 days. The animals were first trained for three trials per day for 3 days with a visible escape platform raised 1 cm above the water line. The interval between each trial was approximately 1 hr. On the fourth training day, the platform was moved to the opposite quadrant of the pool and submerged 1 cm below the surface of the water. The mice were given 5 days of hidden platform training, as well as three trials per day with a 1 hr intertrial interval. A 1 minute probe trial, with the platform removed from the pool, was given 7 days after the last hidden-platform trial. For both visible- and hidden-platform training, every trial began from a different starting position, and the mouse was placed in a beaker facing the wall of the tank. If the mouse did not locate the platform within the allotted time, it was placed on the platform by the experimenter. Mice were left on the platform for 30 s at the end of each trial before being removed from the tank with a large metal spoon and placed under a heat lamp for 5–10 min before being returned to their home cages for 1 hour before the next trial. Swim times and distances during training, as well as probe-trial parameters, were collected with ANY-maze software. Statistical analysis was performed with a two-way repeated-measures ANOVA (genotype  $\times$  trials) followed by a Bonferroni posttest to analyze escape latencies in visible- and hidden-platform testing. A two-way ANOVA (genotype  $\times$  quadrants) followed by a Bonferroni posttest was used to analyze the time spent in each quadrant during the first trial of hidden-platform testing and for the probe trial. For fear conditioning, mice were placed on the first day in a test chamber (30.5 cm length  $\times$  24.1 cm width  $\times$  21.0 cm height, Standard Modular Test Chamber ENV-008, Med Associates) for a conditioning session of 4 min 90 s of habituation, a 2 s foot shock (0.5 mA), 90 s of no stimuli, another foot shock, and a final 60 s of no stimuli. Twenty-four hours after the conditioning session, mice were placed in the test chamber again for 5 min for testing contextual fear conditioning. The percentage of time spent freezing was quantified by video image analysis (Freeze Frame, Coulbourn Instruments) and ANOVA. After the fear-conditioning test, foot-shock-sensitivity testing was performed as outlined in Figure S9.

Depression-related behavior was tested by sucrose preference (a test for anhedonia) and the forced swim test, whereas balance and mobility were tested by an accelerating-rotarod test. Detailed methodology of these three tests is provided in Figure S7.

## Results

### Individuals with De Novo Mutations in *DEAF1*

Upon the identification of two separate de novo mutations in *DEAF1* by trio-based exome sequencing in two independent cohorts encompassing 10 and 51 individuals with

**Table 1. Molecular and Clinical Details of Individuals with *DEAF1* Mutations**

<b>Molecular and Clinical Details</b>	<b>Individual 1<sup>4</sup></b>	<b>Individual 2<sup>2</sup></b>	<b>Individual 3</b>	<b>Individual 4</b>
Gender	male	female	male	female
Age at last visit	9 years	7 years	10 years	10 years
Parental age	mother, 32 years father, 35 years	mother, 31 years father, 32 years	mother, 29 years father, 30 years	mother, 40 years father, 48 years
<b>Mutations</b>				
Amino acid change <sup>a</sup>	p.Ile228Ser	p.Gln264Pro	p.Arg224Trp	p.Arg254Ser
cDNA change <sup>b</sup>	c.683T>G	c.791A>C	c.670C>T	c.762A>C
Chromosome position <sup>c</sup>	chr11: 686,979	chr11: 686,871	chr11: 686,992	chr11: 686,900
PhyloP <sup>26</sup>	4.4	2.5	3.4	-0.4 <sup>d</sup>
SNPs&GO <sup>27</sup>	disease related	disease related	disease related	disease related
MutPred <sup>28</sup>	0.825	0.659	0.551	0.539
PolyPhen-2 <sup>29</sup>	0.984	0.972	0.996	0.999
<b>Growth</b>				
Birth weight (g)	-2 SDs	-0.5 SD	+0.7 SD	NR
Height (cm)	-1.3 SDs	-0.6 SD	-0.4 SD	-1.7 SDs
Weight (kg)	+0.5 SD	-1.5 SDs	-0.8 SD	0 SD
Head circumference (cm)	-0.6 SD	+0.1 SD	-1 SD	+0.3 SD
<b>Development</b>				
Motor delay	mild	mild	mild	mild
Expressive speech <sup>e</sup>	absent	ten single words	absent	disappeared at 18 months
Intellectual disability	severe	moderate	severe	severe
Regression	-	-	+	+
<b>Neurological</b>				
Contact	poor eye contact	good	poor eye contact	poor eye contact
Hypotonia	-	+	-	-
Behavioral problems	+	-	+	+
Autism	+	-	+	+
Mood swings	+	-	+	+
Fascinations	+	NR	NR	+
High pain threshold	+	in childhood	+	+
Sleeping problems	-	-	+	+
Abnormal walking pattern	+	+	+	+
Abnormal brain MRI	NR	-	-	+
<b>Facial</b>				
Thin and/or fair hair	+	+	-	+
Straight eyebrows	+	+	+	+
Full nasal tip	+	+	+	+
Cupid's bow in upper lip	-	+	+	+
Full lower lip	+	+	-	+

*(Continued on next page)*

**Table 1. Continued**

<b>Molecular and Clinical Details</b>	<b>Individual 1<sup>4</sup></b>	<b>Individual 2<sup>2</sup></b>	<b>Individual 3</b>	<b>Individual 4</b>
Prominent chin	+	–	+	+
Other	upslant, epicanthic folds	frontal bossing, high palate	brachycephaly, widow's peak, flat face	NR
<b>Extremities</b>				
Fetal finger pads	+	–	+	–
Skin syndactyly in toes 2 and 3	+	+	+	–
Hyperlaxity	+	+	–	–
<b>Other</b>				
Recurrent infections	in childhood	+	+	in childhood
Sacral dimple	–	+	+	–
Other clinical features	scrotal raphe, flat feet	sandal gap	20–40 dB hearing loss, clinodactyly in toes 3 and 4, dry skin	clinodactyly in toes 4 and 5
Other detected gene mutations	NR	<i>DOCK9</i> c.1604C>T (p.Ala535Val) and <i>CDK18</i> c.118C>T (p.Arg40Trp)	<i>SCN2A</i> c.1570C>T (p.Arg524*)	NR

The following abbreviation is used: NR, not reported.

<sup>a</sup>RefSeq NP\_066288.

<sup>b</sup>RefSeq NM\_021008.2.

<sup>c</sup>UCSC Genome Browser hg19.

<sup>d</sup>This base is the third base of a codon.

<sup>e</sup>Speech comprehension was significantly better in all four individuals.

severe ID,<sup>2,4</sup> we performed targeted resequencing of *DEAF1* in an additional cohort of over 2,300 individuals with ID. Here, we identified two additional individuals with a de novo mutation in *DEAF1*, resulting in a total of four individuals with de novo mutations in this gene: c.683T>G (p.Ile228Ser), c.791A>C (p.Gln264Pro), c.670C>T (p.Arg224Trp), and c.762A>C (p.Arg254Ser) (Table 1, Figures 1A and 1B). All children (age range 7–10 years) showed moderate to severe ID with severely affected expressive speech and only mild motor delay (Table 1). All had a happy predisposition, but three had severe behavioral problems consisting of autistic, hyperactive, compulsive, and aggressive behavior with striking mood swings. Other frequently observed abnormalities were recurrent infections, a high pain threshold, and an abnormal walking pattern. All had normal body measurements, only mild dysmorphism (Figure 1A), and no further congenital anomalies.

#### ***DEAF1* mRNA Expression**

qPCR analysis of *DEAF1* mRNA in various human fetal and adult tissues showed that *DEAF1* was expressed more than 30 times higher in fetal and adult brain than in the duodenum (Figure S2C). In addition, qPCR analysis of *Deaf1* mRNA expression in the brain of adult mice showed that *Deaf1* was expressed 5–20× higher in various brain regions than in the liver (Figure S5). Therefore, we used in situ hybridization at various embryonic stages of zebrafish to

study the expression pattern of *deaf1-a* and *deaf1-b*, which share 53% and 36% homology, respectively, with human *DEAF1*. This showed the highest expression in the brain and spinal cord of both orthologs (Figure S2A). Expression quantification by qPCR showed that *deaf1-a* was transiently expressed about three times higher at 24 days post-fertilization (dpf) than at 14 dpf (Figure S2B), whereas expression of *deaf1-b* was very low to absent at all embryonic stages (data not shown).

#### **Functional Consequences of *DEAF1* Mutations**

All four de novo mutations found in these individuals were missense mutations affecting evolutionary conserved amino acids within the SAND domain (Figures 1C and 1D) and were predicted by SNPs&GO,<sup>27</sup> MutPred,<sup>28</sup> and PolyPhen-2<sup>29</sup> to be detrimental to protein function (Table 1). None of these mutations were present in dbSNP v.139, the NHLBI Exome Sequencing Project Exome Variant Server, or our in-house database containing exome data of over 2,000 individuals. In silico modeling by Project HOPE (Have Your Protein Explained)<sup>30</sup> with the mouse putative nuclear protein ortholog (SP110 [Protein Data Bank ID 1UFN], which shares 40% homology with the human *DEAF1* SAND domain) as a template predicted that all four amino acid substitutions might affect SAND domain function either by directly interfering with the DNA-interaction surface or by disturbing the core structure of this domain (Figure 2A). Therefore, we compared the

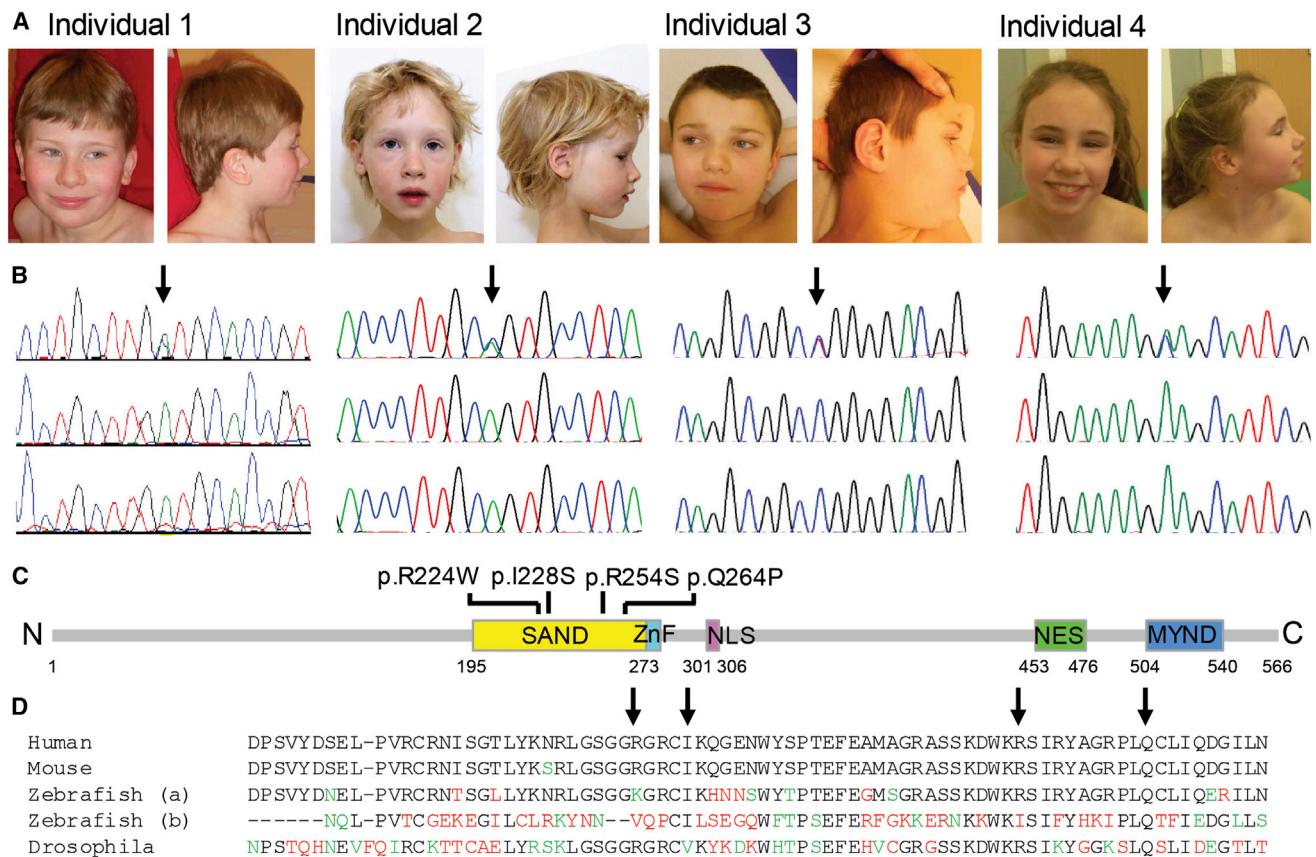


**Figure 1. Individuals with *DEAF1* Mutations**

(A) Frontal and lateral photographs of individuals with *de novo* mutations in *DEAF1*. Only mild facial dysmorphism was observed. (B) Sanger sequencing chromatograms showing the *DEAF1* mutations in the proband (top panel), but not in the parents (bottom panels).

(C) Schematic overview of *DEAF1*, including the known domains (SAND domain, zinc-finger homology [ZnF] domain, nuclear localization signal [NLS], nuclear export signal [NES], and MYND domain). The positions of the four identified missense substitutions (p.Arg224Trp [p. R224W], p.Ile228Ser [p.I228S], p.Arg254Ser [p.R254S], and p.Gln264Pro [p.Q264P]) in the SAND domain are depicted.

(D) Multispecies alignment of the SAND domain in eukaryotes. Amino acid residues with substitutions are indicated by arrows. Amino acids with similar properties are marked in green, and dissimilar amino acids are marked in red. Zebrafish "a" is zgc:194895, and zebrafish "b" is zgc:171506.

functional activities of WT *DEAF1* and of altered *DEAF1* harboring either of the four identified amino acid substitutions along with two previously described alterations affecting the SAND domain.<sup>11</sup>

It was previously shown that *DEAF1* represses its own *DEAF1* promoter and that amino acid substitutions affecting the SAND domain can eliminate DNA binding and promoter repression.<sup>11,12</sup> In a reporter assay with the human *DEAF1* transcriptional promoter fused to a luciferase reporter gene, overexpression of *DEAF1* containing any of the four amino acid substitutions resulted in a loss of the ability to repress the *DEAF1* promoter (Figure 2B). A similar loss of *DEAF1*-promoter repression was observed for the previously characterized combined p.Lys250Ala and p.Lys253Ala substitutions, localized within the essential positively charged surface of the KDWK motif, whereas the randomly selected p.Arg226Ala change, located between the amino acid substitutions identified in this study (p.Arg224Trp and p.Ile228Ser), had no effect on transcriptional repression,<sup>11</sup> indicating that the amino

acid substitutions identified in this study are specifically deleterious.

*DEAF1* has also been shown to function as a transcriptional activator of eukaryotic translation initiation factor 4 gamma, 3 (*Eif4g3* [RefSeq accession number NM\_172703]).<sup>8,10</sup> Relative to basal transcription, WT *DEAF1* produced about a 2-fold activation of the mouse *Eif4g3* reporter construct, whereas the amino acid substitution identified in this study (p.Arg224Trp) showed no activation (Figure 2C). Both amino acid substitutions p.Ile228Ser and p.Gln264Pro showed not only loss of transcriptional activation but also an approximate 10-fold suppression of transcription relative to basal expression levels, whereas the amino acid substitution identified in this study (p.Arg254Ser) and the randomly selected substitution p.Arg226Ala continued to activate *Eif4g3* reporter expression.

Because the SAND domain mediates *DEAF1* DNA binding, we performed EMSAs to examine whether impaired DNA binding could underlie the impaired transcriptional

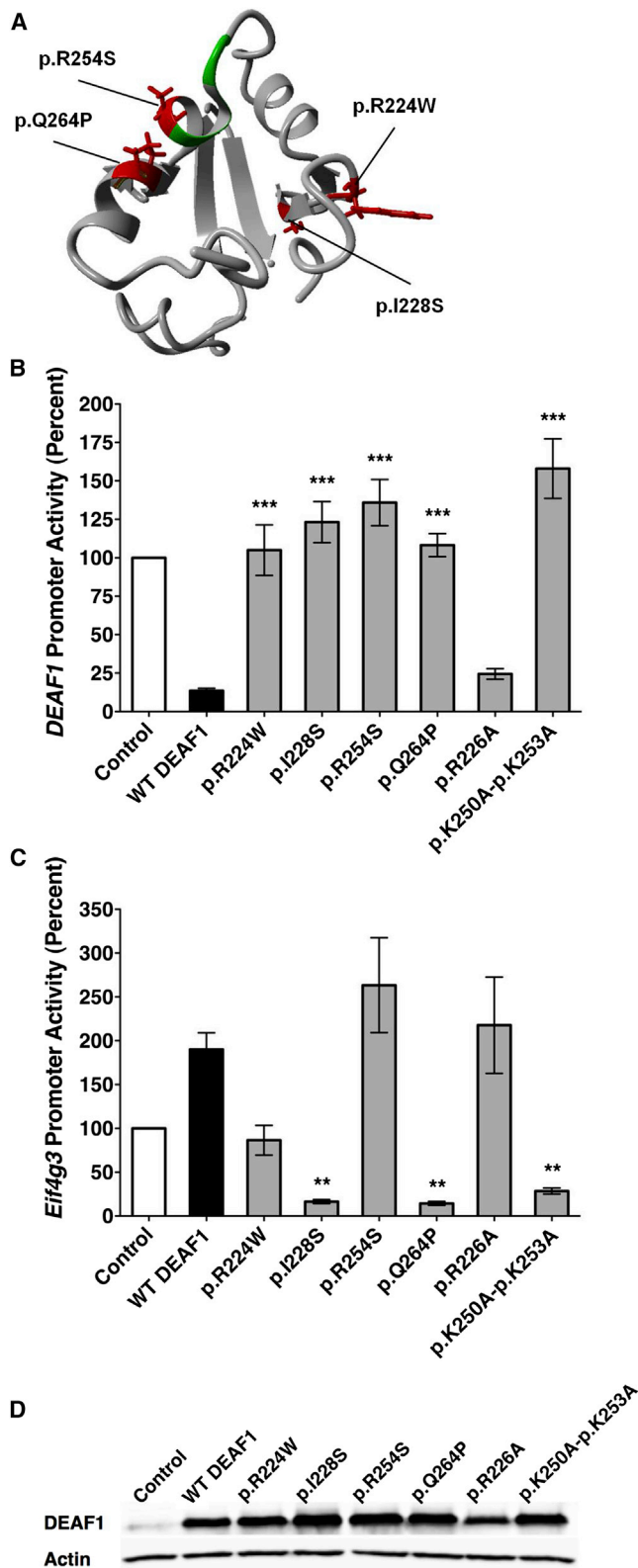


**Figure 2. DEAF1 Mutations Alter Transcriptional Regulation**  
 (A) This 3D model of the SAND domain is based on the homologous structure from the mouse putative nuclear protein homolog (SP110); the four amino acid substitutions are in red, and the essential KDWK motif is in green.  
 (B) DEAF1 promoter activity after transfection with either WT or altered FLAG-tagged DEAF1. Similar to the previously character-

regulation. For DEAF1, we utilized two DNA ligands, one based on a sequence found in the human DEAF1 promoter<sup>11,12</sup> and one based on the preferred binding motif of DEAF1 (data not shown; Table S1). Recombinant DEAF1 containing the amino acid substitutions identified in this study (p.Arg224Trp, p.Ile228Ser, and p.Gln264Pro) showed a complete loss of DNA binding to both DNA ligands, whereas p.Arg254Ser altered DEAF1 displayed a 9-fold reduction in binding of the DNA ligand with 11 bp CG-spacing and a 53-fold reduction in the DNA ligand with 6 bp CG spacing (Figure 3A). Thus, all four of the ID-associated mutations produce proteins with loss of or highly reduced DNA binding.

The SAND domain of DEAF1 also mediates DEAF1 multimerization, which is required for DNA binding.<sup>15</sup> We have previously demonstrated that DEAF1-DEAF1 interactions can be monitored by immunofluorescence and a relocalization of a cytoplasmically localized p.Lys304Thr altered DEAF1 to the nucleus.<sup>15</sup> p.Arg224Trp, p.Ile228Ser, p.Arg254Ser, and p.Gln264Pro altered DEAF1 showed normal localization to the nucleus, and they were all able to relocalize the p.Lys304Thr altered DEAF1 from the cytoplasm to the nucleus (Figure 3C).

The SAND domain of DEAF1 also mediates interaction with X-ray repair cross-complementing protein 6 (XRCC6, also called Ku70 [RefSeq NP\_001275905]), which is a subunit of the DNA-dependent protein kinase complex.<sup>14</sup> Using GST-pull-down assays, we showed that the interaction with XRCC6 was greatly reduced for both amino acid substitutions p.Ile228Ser and p.Gln264Pro and mildly reduced for substitution p.Arg224Trp, but XRCC6 interaction with substitution p.Arg254Ser was retained (Figure 3B), indicating that for these substitutions, SAND domain function seems further compromised.

ized combined p.Lys250Ala and p.Lys253Ala substitutions, the substitutions identified in this study (p.Arg224Trp [p.R224W], p.Ile228Ser [p.I228S], p.Arg254Ser [p.R254S], and p.Gln264Pro [p.Q264P]) were unable to repress DEAF1 promoter activity. The p.Arg226Ala (p.R226A) substitution had no effect on transcriptional repression. Each bar represents the mean  $\pm$  SEM of the normalized luciferase activity of three independent experiments when the activity of pcDNA3 (DEAF1 promoter alone) was set to 100%. One-way ANOVA with both Dunnett's multiple comparison and selected Bonferroni posttest of WT DEAF1 versus each mutant, \*\*\* $p$  < 0.001.

(C) Promoter activity of mouse Eif4g3 after transfection with either WT or altered FLAG-tagged DEAF1. Relative to basal transcription, WT DEAF1 and p.Arg254Ser altered DEAF1 produced about a 2-fold activation of the reporter construct, whereas the p.Arg224Trp altered DEAF1 showed no activation. Both the p.Ile228Ser and the p.Gln264Pro proteins showed not only a loss of transcriptional activation but also an approximately 10-fold suppression of transcription relative to basal expression levels. The results are from three independent experiments and analyzed as in (B). \*\* $p$  < 0.01.  
 (D) Immunoblot analysis for transfected amounts of FLAG-tagged DEAF1 in HEK293T cells. Equal quantities of transfected cell lysates were assayed for WT and altered FLAG-tagged DEAF1 with the use of anti-DEAF1 antibody (anti-actin antibody was used as a loading control). DEAF1 amounts were similar in the transfected cell lysates.

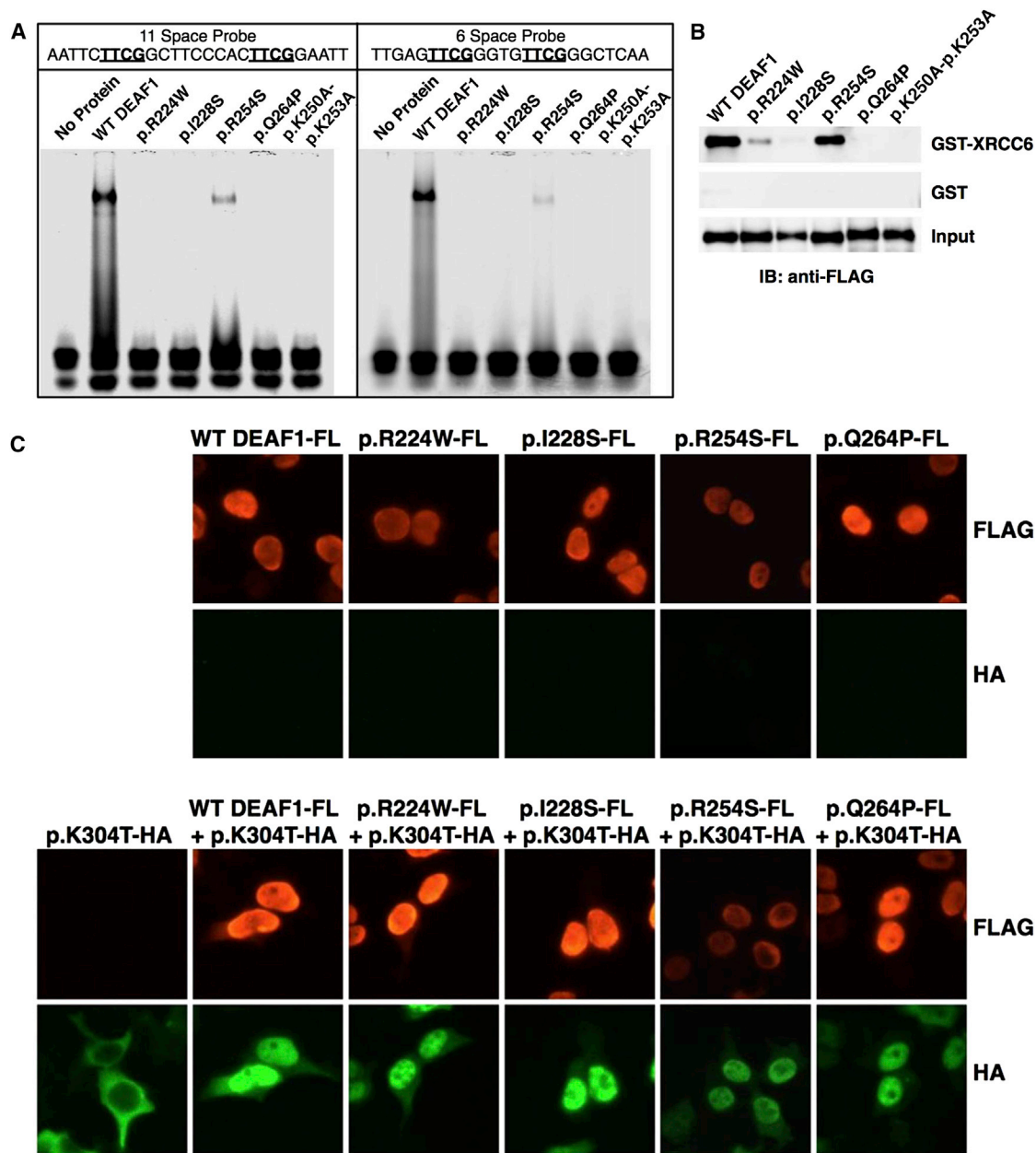


**Figure 3. DEAF1 Mutations Alter DNA and Protein Interactions**

(A) EMSA of WT and altered FLAG-tagged DEAF1 recombinant proteins isolated from HEK293T cells. Fluorescently labeled DNA ligands with a spacing of 11 or 6 nucleotides between the CG dinucleotides were examined. The p.Arg224Trp (p.R224W), p.Ile228Ser (p.I228S), and p.Gln264Pro (p.Q264P) proteins lacked DNA binding, whereas the p.Arg254Ser (p.R254S) protein showed less binding than WT DEAF1.

(B) XRCC6 interaction with recombinant FLAG-tagged DEAF1 was assessed in GST pull-downs. GST-XRCC6 could pull down WT DEAF1 and the p.Arg254Ser protein. The p.Arg224Trp protein had reduced interaction, and the p.Gln264Pro and p.Ile228Ser proteins had no interaction. The GST-only control did not pull down DEAF1. Recombinant proteins were detected with anti-FLAG antibodies.

(C) DEAF1-DEAF1 interaction was assessed in an immunofluorescence assay. HEK293T cells were transfected with expression plasmids for WT or altered FLAG-tagged DEAF1 by themselves or in combination with an expression plasmid for the p.Lys304Thr (p.K304T) DEAF1 with an HA epitope tag and were then assayed for location by immunofluorescence with anti-FLAG or anti-HA antibodies. WT and altered FLAG-tagged DEAF1 localized to the nucleus. The p.Lys304Thr-HA protein localized to the cytoplasm but relocated to the nucleus in the presence of WT or altered DEAF1.

### Behavior Phenotyping of Mice with Conditional Targeting of *Deaf1*

Mice with a targeted disruption of exons 2–5 of *Deaf1* (*Deaf1*<sup>+/-</sup> mice) were produced (Figures S3 and S4). On a C57BL/6 background, *Deaf1*<sup>-/-</sup> neonates died 100% of

the time and *Deaf1*<sup>+/-</sup> mice survived in a 2:1 ratio relative to WT mice (Tables S2–S4), and only 3% of *Deaf1*<sup>-/-</sup> mice survived on a BALB/c background (Table S5), which precluded behavioral studies. Therefore, we created a conditional knockout model of *Deaf1* in mouse brain by



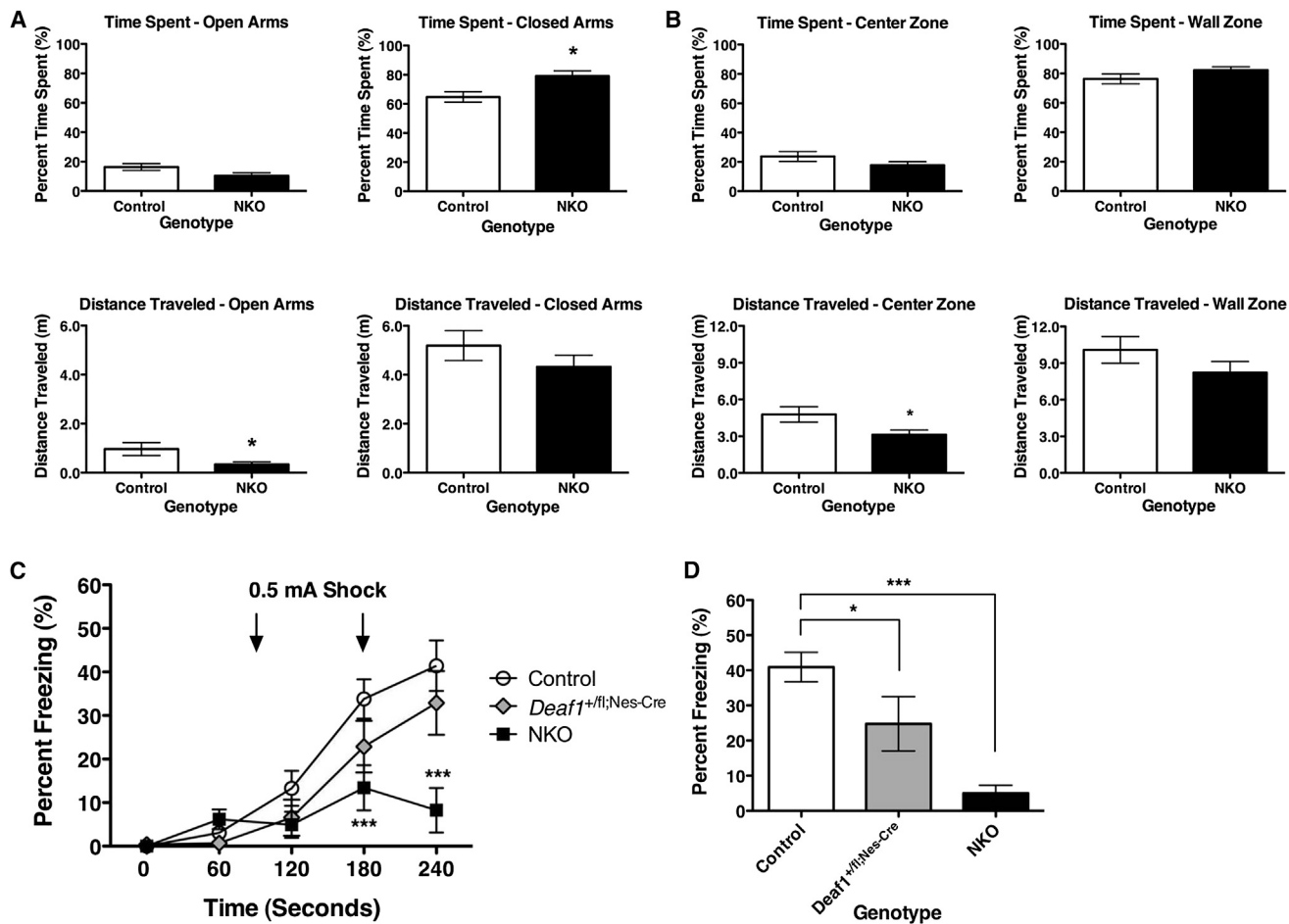


**Figure 4. Behavioral Phenotyping of Mice with Conditional Knockout of *Deaf1* in the Brain**

(A) Anxiety testing using the EPM. Bars represent the mean  $\pm$  SEM of the time spent or distance traveled in open and closed arms (control mice,  $n = 12$ ; NKO mice,  $n = 12$ ). NKO mice spent significantly more time in the closed arm and traveled significantly less distance in the open arm. Unpaired two-tailed  $t$  test,  $*p < 0.05$ .

(B) Anxiety testing using the open-field test. Bars represent the mean  $\pm$  SEM of the time spent or distance traveled in the center or wall zones (control mice,  $n = 12$ ; NKO mice,  $n = 12$ ). NKO mice displayed significantly reduced distance traveled in the center zone. Unpaired two-tailed  $t$  test,  $*p < 0.05$ .

(C) Percentage of time freezing in response to foot shock. Training on day 1 is shown, and arrows indicate the time of a 0.5 mA shock (control mice,  $n = 18$ ; *Deaf1<sup>+fl</sup>;Nes-cre* mice,  $n = 10$ ; NKO mice,  $n = 14$ ). Bars represent the mean  $\pm$  SEM. NKO mice displayed significantly reduced freezing at 180 and 240 s. Two-way repeated-measures ANOVA with Bonferroni posttest between control and NKO mice,  $***p < 0.001$ .

(D) Percentage of time freezing in contextual fear conditioning. Context testing 24 hr after training is shown (control mice,  $n = 18$ ; *Deaf1<sup>+fl</sup>;Nes-cre* mice,  $n = 10$ ; NKO mice,  $n = 14$ ). Bars represent the average of 5 min  $\pm$  SEM. NKO and *Deaf1<sup>+fl</sup>;Nes-cre* mice displayed significantly reduced freezing. One-way ANOVA with Bonferroni posttest,  $*p < 0.05$ ,  $***p < 0.001$ .

breeding mice with loxP sites flanking exons 2–5 of *Deaf1* (*Deaf1<sup>+fl</sup>*) to mice transgenic for *Nes-cre*. NKO mice survived to adulthood at levels similar to those of WT mice, and various brain regions showed 11- to 49-fold reductions of the WT *Deaf1* mRNA transcript (Figure S5).

Adult male mice (median age 4 months) consisting of NKO, *Deaf1<sup>+fl</sup>;Nes-cre*, and control genotypes were sequentially tested with two anxiety tests (the EPM and the open-field test) followed by two tests for depression-related behavior (the sucrose-preference test, which tests for anhedonia, and the forced-swim test). In addition, a second group of adult male mice (median age 7 months) was tested for changes in balance and mobility with an accelerating-rotarod test. In anxiety tests, NKO mice spent statis-

tically significantly more time in the closed arms (NKO mice =  $79.0\% \pm 3.7\%$  versus control mice =  $64.7\% \pm 3.6\%$ ,  $p < 0.05$ ) and showed less distance traveled on the open arms of the EPM than did control mice (NKO mice =  $0.34 \pm 0.10$  m versus control mice =  $0.97 \pm 0.26$  m,  $p < 0.05$ ; Figure 4A). NKO mice also displayed less distance traveled in the center zone of the open field than did controls (NKO mice =  $3.12 \pm 0.38$  m versus control mice =  $4.77 \pm 0.63$  m,  $p < 0.05$ ; Figure 4B). Distance traveled in the closed arms of the EPM and the wall zone of the open field was similar between the two genotypes, indicating that the NKO mice did not have mobility deficiencies. Relative to control mice, conditional heterozygous mice (*Deaf1<sup>+fl</sup>;Nes-cre*) did not display any behavior

differences in the anxiety tests (Figure S6). No differences were observed between NKO and control mice for depression-like behavior in the sucrose-preference and forced-swim tests (Figures S7A and S7B) or for rotarod performance (Figure S7C).

### Learning and Memory in Mice with Conditional Knockout of *Deaf1*

A group of adult male mice (median age 7 months) was evaluated for changes in learning and memory with the Morris water maze and fear-conditioning testing. All three genotypes showed similar learning curves when they tried to find a visible platform in the Morris water maze (Figure S8A). When mice were retested 48 hr later, NKO mice were significantly faster than control mice at finding a hidden (submerged) platform that had been moved to the opposite quadrant (NKO mice =  $42.3 \pm 9.3$  s versus control mice =  $80.3 \pm 6.7$  s,  $p < 0.001$ ), but only on the first trial with the hidden platform (Figures S8B and S8C). Thereafter, learning curves for the hidden platform were similar among the three genotypes (Figure S8B). When mice were tested with a probe trial 7 days later, no difference in long-term memory was observed (Figure S8D).

Mice were then tested in a contextual fear-conditioning task, wherein the mice were placed into a novel environment and given an electrical foot shock to induce fear memory, as demonstrated by behavioral freezing. NKO mice showed reduced freezing behavior in response to a foot shock (at 240 s, NKO mice =  $8.2\% \pm 5.1\%$  versus control mice =  $41.4\% \pm 5.8\%$ ,  $p < 0.001$ ; Figure 4C), and both NKO mice and conditional heterozygous *Deaf1*<sup>+/*fl*</sup>;*Nes-cre* mice displayed significantly reduced contextual fear memory 24 hr later (NKO mice =  $5.0\% \pm 2.3\%$  and *Deaf1*<sup>+/*fl*</sup>;*Nes-cre* mice =  $24.6\% \pm 7.7\%$  versus control mice =  $40.9\% \pm 4.2\%$ ; Figure 4D). Given that individuals with de novo mutations in *DEAF1* showed increased pain tolerance, a potential explanation for the response in fear conditioning might be a reduced ability to feel the foot shock. However, relative to controls, NKO mice did not display diminished responses to increasing levels of foot shock (Figure S9).

### Discussion

Novel sequencing techniques have identified de novo mutations in candidate genes for genetically heterogeneous disorders such as ID. Correlating the clinical consequence of such mutations in these candidate genes is, however, challenging and relies on the identification of additional individuals with mutations affecting the same gene and an overlapping phenotype and functional assays. Here, we describe de novo missense mutations affecting the SAND domain of *DEAF1* in four individuals with ID, severe speech impairment, and behavioral problems. We showed that all four of the amino acid substitutions impaired the

normal function of *DEAF1* in transcriptional regulation of the *DEAF1* promoter and produced loss or greatly reduced binding of DNA ligands. Furthermore, we observed that *DEAF1* was highly expressed in the CNS and that neuronal knockout of *Deaf1* in mice resulted in increased anxiety and deficits in learning and memory. In this way, we have provided further evidence of a causal role for de novo mutations affecting the SAND domain of *DEAF1* in the phenotype observed in these individuals.

The phenotype of the individuals with *DEAF1* mutations consisted of moderate to severe ID, disproportionately severely affected expressive speech (but significantly better speech comprehension and motor development), and behavioral problems. Two of the four subjects were identified in preselected cohorts of individuals with moderate to severe ID.<sup>2,4</sup> The other two subjects, however, were identified in a cohort of over 2,300 individuals with unexplained ID (an unselected cohort with the full phenotypic spectrum of individuals with ID), indicating that the ascertainment of these latter individuals was not subjected to selection bias. Because large-scale resequencing efforts have only focused on high-quality variant calls, potentially leaving some true mutations undetected, the true incidence of *DEAF1* mutations affecting the SAND domain of *DEAF1* in an unbiased cohort of individuals with ID remains to be determined.

Angelman syndrome (MIM 105830) was considered in the differential diagnosis for all four individuals on the basis of their severely impaired speech development, happy predisposition, fascination with water, and coordination problems, but a diagnostic methylation study of the 15q11–q13 region and/or mutation analysis of *UBE3A* (MIM 601623) gave normal results. In addition, all four individuals were susceptible to recurrent infections, which might be explained by the role of *DEAF1* in interferon  $\beta$  gene transcription through interaction with interferon regulatory factor 3.<sup>31</sup> The behavioral abnormalities present in three of the four individuals consisted of autistic, hyperactive, and aggressive behavior with striking mood swings. Because *DEAF1* has previously been linked to major depression and suicide through regulation of 5-hydroxytryptamine receptor 1A,<sup>20–22</sup> disturbance of the serotonin pathway might contribute to the phenotypes seen in the individuals reported here. Interestingly, in addition to the *DEAF1* mutation in the second individual, other candidate mutations were identified. The overlapping phenotype between this girl and the other individuals with mutations in *DEAF1* indicates that the mutation in *DEAF1* is the underlying cause.

We observed a high expression of *DEAF1* mRNA in the CNS in both humans and mice, as well as in zebrafish. This expression was observed in both fetal and adult human brain, whereas in zebrafish, *deaf1* expression was highest at earlier developmental stages. *Deaf1* has been previously reported to be widely expressed in mouse and rat tissues, as well as highly expression in the CNS.<sup>6,32,33</sup>

The expression of *DEAF1* at the high level found in the CNS might explain why mainly the nervous system is affected in these individuals.

We aimed to determine whether the different amino acid substitutions observed in the individuals with ID compromised normal functioning of DEAF1. All four de novo mutations altered the SAND domain, suggesting that these might result in inappropriate functioning of this domain. We tested the effect of the amino acid substitutions on three essential functions of the SAND domain, namely DNA binding, transcription regulation, and SAND-domain-mediated protein interactions. All four substitutions showed loss of transcriptional repression of the *DEAF1* promoter, indicating that all mutations identified in this study impair the normal function of *DEAF1* in transcriptional repression. In addition, three of the substitutions showed complete loss of DNA binding, and one showed greatly reduced DNA binding. Three of the four amino acid substitutions failed to activate the *Eif4g3* promoter, and two of them even resulted in a 10-fold suppression of transcription relative to basal expression levels. Three of the four substitutions also resulted in reduced interaction with XRCC6, indicating that for these substitutions, SAND domain function seems further compromised.

The impaired repression of the *DEAF1* promoter indicates that the de novo mutations as seen in these individuals could impair the normal function of DEAF1 by a loss-of-function effect. Contradictory to this hypothesis, however, is the observation that deletions including *DEAF1* have been reported for healthy controls<sup>34</sup> and that we identified a 1 bp insertion (chr11: g.674717del) leading to a frameshift (p.Leu441Trpfs\*16) in *DEAF1* in a healthy individual (data not shown). Therefore, a more likely mechanism explaining the consequences of these *DEAF1* mutations might be a dominant-negative effect. Data that support this hypothesis are that all of the altered forms of DEAF1 were able to interact with a cytoplasmically localized DEAF1 and relocalize it to the nucleus and that two of the altered proteins produced dominant-negative activity in the transcriptional activation of *Eif4g3*. In previous large-scale exome sequencing studies, the importance of loss-of-function mutations was stressed,<sup>35,36</sup> but here we show the importance and clinical relevance of missense mutations most likely caused by effects different from loss of function.

Because the de novo mutations identified in individuals with ID most likely have dominant-negative activity, incapacitating both copies of *DEAF1*, we hypothesized that knockout of *Deaf1* in mice would result in behavior disorders. To test this hypothesis, we produced mice with a targeted disruption of *Deaf1*. Because our full knockout of *Deaf1* was embryonically lethal, we utilized a conditional knockout of *Deaf1* in the brain to perform studies on large enough cohorts of mice to obtain behavioral data. Partial survival of another *Deaf1*-knockout mouse was previously reported.<sup>18</sup> The increased lethality in our knockout mice could be due to strain differences, or the other mouse

model could represent mice with partial retention of *Deaf1* function.

Mice with conditional homozygous knockout of *Deaf1* in neuronal tissues showed increased anxiety in the EPM and the open-field test. The increased anxiety behavior of the NKO mice might be relevant to the behavioral abnormalities observed in individuals with de novo *DEAF1* mutations. Fear-conditioning tests demonstrated a deficiency of NKO mice to freeze in response to foot shock, which additional testing indicated was unlikely to be due to diminished pain sensitivity, inferring that it might be related to an increased anxiety response of the mice. Compared to WT mice, both NKO and conditional heterozygous mice showed a lack of contextual memory in the fear-conditioning test after 24 hr. The memory deficits in the NKO mice might have relevance to higher-order cognitive deficiencies of individuals with ID. The observation that conditional heterozygous knockout mice also had memory deficits provides supporting evidence that the de novo *DEAF1* mutations observed in these heterozygous individuals might result in ID.

In conclusion, we show that de novo mutations affecting the SAND domain of the transcription factor DEAF1 cause a human phenotype characterized by ID with severe speech impairment and behavioral problems and provide various functional evidence that links dysregulation of *DEAF1* to the observed phenotype. Over the coming years, we expect many more mutations in *DEAF1* to be identified. Therefore, we established a website to collect detailed phenotypic data of individuals harboring *DEAF1* mutations not only to gain insight into the clinical spectrum that these mutations might cause but also to obtain fundamental understanding of the pathogenic mechanisms underlying *DEAF1*-related ID.

### Supplemental Data

Supplemental Data include nine figures and five tables and can be found with this article online at <http://dx.doi.org/10.1016/j.ajhg.2014.03.013>.

### Acknowledgments

We are grateful to the individuals involved and their parents for their participation. We would like to thank Hanka Venselaar for the in silico modeling of the *DEAF1* mutations. This work was supported by European Commission GENCODYS grant 241995 under the Seventh Framework Programme (to A.T.V.v.S. and B.B.A.d.V.), Netherlands Organisation for Health Research and Development grants 917-86-319 (to B.B.A.d.V.), 912-12-109 (to B.B.A.d.V. and J.A.V.), and 916-12-095 (to A.H.), NIH grants CA89438, CA137556, and HD060122 (to J.I.H. and M.W.C.), funds from the Southern Illinois University School of Medicine (to J.I.H. and M.W.C.), and funds from the Fraternal Order of Eagles in Carbonale (to J.I.H. and M.W.C.).

Received: January 29, 2014

Accepted: March 18, 2014

Published: April 10, 2014

## Web Resources

The URLs for data presented herein are as follows:

Database of Genomic Variants, <http://projects.tcag.ca/variation/>  
DEAF1 clinical website, <http://www.deaf1gene.com>  
DECIPHER, <http://decipher.sanger.ac.uk/>  
NHLBI Exome Sequencing Project (ESP) Exome Variant Server, <http://evs.gs.washington.edu/>  
Online Mendelian Inheritance in Man (OMIM), <http://www.omim.org>  
Project HOPE, <http://www.cmbi.ru.nl/hope/home>  
RefSeq, <http://www.ncbi.nlm.nih.gov/RefSeq>  
UCSC Genome Browser, <http://genome-euro.ucsc.edu/cgi-bin/hgGateway?redirect=auto&source=genome.ucsc.edu>

## References

- de Ligt, J., Willemsen, M.H., van Bon, B.W., Kleefstra, T., Yntema, H.G., Kroes, T., Vulto-van Silfhout, A.T., Koolen, D.A., de Vries, P., Gilissen, C., et al. (2012). Diagnostic exome sequencing in persons with severe intellectual disability. *N. Engl. J. Med.* 367, 1921–1929.
- Rauch, A., Wieczorek, D., Graf, E., Wieland, T., Ende, S., Schwarzmayr, T., Albrecht, B., Bartholdi, D., Beygo, J., Di Donato, N., et al. (2012). Range of genetic mutations associated with severe non-syndromic sporadic intellectual disability: an exome sequencing study. *Lancet* 380, 1674–1682.
- Veltman, J.A., and Brunner, H.G. (2012). De novo mutations in human genetic disease. *Nat. Rev. Genet.* 13, 565–575.
- Vissers, L.E., de Ligt, J., Gilissen, C., Janssen, I., Steehouwer, M., de Vries, P., van Lier, B., Arts, P., Wieskamp, N., del Rosario, M., et al. (2010). A de novo paradigm for mental retardation. *Nat. Genet.* 42, 1109–1112.
- Yang, Y., Muzny, D.M., Reid, J.G., Bainbridge, M.N., Willis, A., Ward, P.A., Braxton, A., Beuten, J., Xia, F., Niu, Z., et al. (2013). Clinical whole-exome sequencing for the diagnosis of mendelian disorders. *N. Engl. J. Med.* 369, 1502–1511.
- Huggenvik, J.I., Michelson, R.J., Collard, M.W., Ziemba, A.J., Gurley, P., and Mowen, K.A. (1998). Characterization of a nuclear deformed epidermal autoregulatory factor-1 (DEAF-1)-related (NUDR) transcriptional regulator protein. *Mol. Endocrinol.* 12, 1619–1639.
- Yip, L., Su, L., Sheng, D., Chang, P., Atkinson, M., Czesak, M., Albert, P.R., Collier, A.R., Turley, S.J., Fathman, C.G., and Creusot, R.J. (2009). Deaf1 isoforms control the expression of genes encoding peripheral tissue antigens in the pancreatic lymph nodes during type 1 diabetes. *Nat. Immunol.* 10, 1026–1033.
- Barker, H.E., Smyth, G.K., Wettenhall, J., Ward, T.A., Bath, M.L., Lindeman, G.J., and Visvader, J.E. (2008). Deaf-1 regulates epithelial cell proliferation and side-branching in the mammary gland. *BMC Dev. Biol.* 8, 94.
- Gross, C.T., and McGinnis, W. (1996). DEAF-1, a novel protein that binds an essential region in a Deformed response element. *EMBO J.* 15, 1961–1970.
- Yip, L., Creusot, R.J., Pager, C.T., Sarnow, P., and Fathman, C.G. (2013). Reduced DEAF1 function during type 1 diabetes inhibits translation in lymph node stromal cells by suppressing Eif4g3. *J. Mol. Cell Biol.* 5, 99–110.
- Bottomley, M.J., Collard, M.W., Huggenvik, J.I., Liu, Z., Gibson, T.J., and Sattler, M. (2001). The SAND domain structure defines a novel DNA-binding fold in transcriptional regulation. *Nat. Struct. Biol.* 8, 626–633.
- Michelson, R.J., Collard, M.W., Ziemba, A.J., Persinger, J., Bartholomew, B., and Huggenvik, J.I. (1999). Nuclear DEAF-1-related (NUDR) protein contains a novel DNA binding domain and represses transcription of the heterogeneous nuclear ribonucleoprotein A2/B1 promoter. *J. Biol. Chem.* 274, 30510–30519.
- Gibson, T.J., Ramu, C., Gemünd, C., and Aasland, R. (1998). The APECED polyglandular autoimmune syndrome protein, AIRE-1, contains the SAND domain and is probably a transcription factor. *Trends Biochem. Sci.* 23, 242–244.
- Jensik, P.J., Huggenvik, J.I., and Collard, M.W. (2012). Deformed epidermal autoregulatory factor-1 (DEAF1) interacts with the Ku70 subunit of the DNA-dependent protein kinase complex. *PLoS ONE* 7, e33404.
- Jensik, P.J., Huggenvik, J.I., and Collard, M.W. (2004). Identification of a nuclear export signal and protein interaction domains in deformed epidermal autoregulatory factor-1 (DEAF-1). *J. Biol. Chem.* 279, 32692–32699.
- Kateb, F., Perrin, H., Tripsianes, K., Zou, P., Spadaccini, R., Bottomley, M., Franzmann, T.M., Buchner, J., Ansieau, S., and Sattler, M. (2013). Structural and functional analysis of the DEAF-1 and BS69 MYND domains. *PLoS ONE* 8, e54715.
- Cubeddu, L., Joseph, S., Richard, D.J., and Matthews, J.M. (2012). Contribution of DEAF1 structural domains to the interaction with the breast cancer oncogene LMO4. *PLoS ONE* 7, e39218.
- Hahm, K., Sum, E.Y., Fujiwara, Y., Lindeman, G.J., Visvader, J.E., and Orkin, S.H. (2004). Defective neural tube closure and anteroposterior patterning in mice lacking the LIM protein LMO4 or its interacting partner Deaf-1. *Mol. Cell. Biol.* 24, 2074–2082.
- Veraksa, A., Kennison, J., and McGinnis, W. (2002). DEAF-1 function is essential for the early embryonic development of *Drosophila*. *Genesis* 33, 67–76.
- Czesak, M., Le François, B., Millar, A.M., Deria, M., Daigle, M., Visvader, J.E., Anisman, H., and Albert, P.R. (2012). Increased serotonin-1A (5-HT1A) autoreceptor expression and reduced raphe serotonin levels in deformed epidermal autoregulatory factor-1 (Deaf-1) gene knock-out mice. *J. Biol. Chem.* 287, 6615–6627.
- Lemondé, S., Turecki, G., Bakish, D., Du, L., Hrdina, P.D., Bown, C.D., Sequeira, A., Kushwaha, N., Morris, S.J., Basak, A., et al. (2003). Impaired repression at a 5-hydroxytryptamine 1A receptor gene polymorphism associated with major depression and suicide. *J. Neurosci.* 23, 8788–8799.
- Szewczyk, B., Albert, P.R., Burns, A.M., Czesak, M., Overholser, J.C., Jurjus, G.J., Meltzer, H.Y., Konick, L.C., Dieter, L., Herbst, N., et al. (2009). Gender-specific decrease in NUDR and 5-HT1A receptor proteins in the prefrontal cortex of subjects with major depressive disorder. *Int. J. Neuropsychopharmacol.* 12, 155–168.
- Manne, U., Gary, B.D., Oelschläger, D.K., Weiss, H.L., Frost, A.R., and Grizzle, W.E. (2001). Altered subcellular localization of suppressin, a novel inhibitor of cell-cycle entry, is an independent prognostic factor in colorectal adenocarcinomas. *Clin. Cancer Res.* 7, 3495–3503.
- O’Roak, B.J., Vives, L., Fu, W., Egerton, J.D., Stanaway, I.B., Phelps, I.G., Carvill, G., Kumar, A., Lee, C., Ankenman, K., et al. (2012). Multiplex targeted sequencing identifies recurrently mutated genes in autism spectrum disorders. *Science* 338, 1619–1622.

25. Tronche, F., Kellendonk, C., Kretz, O., Gass, P., Anlag, K., Orban, P.C., Bock, R., Klein, R., and Schütz, G. (1999). Disruption of the glucocorticoid receptor gene in the nervous system results in reduced anxiety. *Nat. Genet.* *23*, 99–103.
26. Pollard, K.S., Hubisz, M.J., Rosenbloom, K.R., and Siepel, A. (2010). Detection of nonneutral substitution rates on mammalian phylogenies. *Genome Res.* *20*, 110–121.
27. Calabrese, R., Capriotti, E., Fariselli, P., Martelli, P.L., and Casadio, R. (2009). Functional annotations improve the predictive score of human disease-related mutations in proteins. *Hum. Mutat.* *30*, 1237–1244.
28. Li, B., Krishnan, V.G., Mort, M.E., Xin, F., Kamati, K.K., Cooper, D.N., Mooney, S.D., and Radivojac, P. (2009). Automated inference of molecular mechanisms of disease from amino acid substitutions. *Bioinformatics* *25*, 2744–2750.
29. Adzhubei, I.A., Schmidt, S., Peshkin, L., Ramensky, V.E., Gerasimova, A., Bork, P., Kondrashov, A.S., and Sunyaev, S.R. (2010). A method and server for predicting damaging missense mutations. *Nat. Methods* *7*, 248–249.
30. Venselaar, H., Te Beek, T.A., Kuipers, R.K., Hekkelman, M.L., and Vriend, G. (2010). Protein structure analysis of mutations causing inheritable diseases. An e-Science approach with life scientist friendly interfaces. *BMC Bioinformatics* *11*, 548.
31. Ordureau, A., Enesa, K., Nanda, S., Le Francois, B., Pegg, M., Prescott, A., Albert, P.R., and Cohen, P. (2013). DEAF1 is a Pellino1-interacting protein required for interferon production by Sendai virus and double-stranded RNA. *J. Biol. Chem.* *288*, 24569–24580.
32. LeBoeuf, R.D., Ban, E.M., Green, M.M., Stone, A.S., Propst, S.M., Blalock, J.E., and Tauber, J.D. (1998). Molecular cloning, sequence analysis, expression, and tissue distribution of suppressin, a novel suppressor of cell cycle entry. *J. Biol. Chem.* *273*, 361–368.
33. Zhang, J., Moseley, A., Jegga, A.G., Gupta, A., Witte, D.P., Sartor, M., Medvedovic, M., Williams, S.S., Ley-Ebert, C., Coolen, L.M., et al. (2004). Neural system-enriched gene expression: relationship to biological pathways and neurological diseases. *Physiol. Genomics* *18*, 167–183.
34. Iafrate, A.J., Feuk, L., Rivera, M.N., Listewnik, M.L., Donahoe, P.K., Qi, Y., Scherer, S.W., and Lee, C. (2004). Detection of large-scale variation in the human genome. *Nat. Genet.* *36*, 949–951.
35. O’Roak, B.J., Vives, L., Girirajan, S., Karakoc, E., Krumm, N., Coe, B.P., Levy, R., Ko, A., Lee, C., Smith, J.D., et al. (2012). Sporadic autism exomes reveal a highly interconnected protein network of de novo mutations. *Nature* *485*, 246–250.
36. Sanders, S.J., Murtha, M.T., Gupta, A.R., Murdoch, J.D., Raubeson, M.J., Willsey, A.J., Ercan-Sencicek, A.G., DiLullo, N.M., Parikshak, N.N., Stein, J.L., et al. (2012). De novo mutations revealed by whole-exome sequencing are strongly associated with autism. *Nature* *485*, 237–241.